Determination of Beach Sand Parameters Using Remotely Sensed Aircraft Reflectance Data

ROBERT A SHUCHMAN

Environmental Research Institute of Michigan, P O Box 8618, Ann Arbor, Michigan 48107

and

DAVID K REA

Department of Atmospheric and Oceanic Science, The University of Michigan, Ann Arbor, Michigan 48109

An algorithm was developed which determines the mineralogy, moisture, and grain size of beach sands based on the hemispherical reflectance in 17 discrete spectral bands The bands chosen range between 0 40 and 2 5 μm, a wavelength range practical for existing multispectral remote sensing technology The sand spectra on which the mineralogy, moisture, and grain-size algorithm (MOGS) is based were obtained from laboratory spectrophotometric measurements Selected spectral bands are used in a vector-length-decision framework to determine the mineralogical class of the input sand Multiple linear regressions are then used, within a given mineralogical class, to determine the moisture and grain size of the sand The predictive results of the MOGS algorithm are very encouraging When tested on 70 of the sand reflectance spectra from which it was derived, the correlation of actual to predicted moisture and grain size was 96% and 88%, respectively The MOGS algorithm has been successfully tested using aircraft multispectral scanner data collected over the Lake Michigan shoreline The algorithm correctly identified gross mineralogy and predicted grain size to within 0 09 mm of measured values Some difficulties were encountered in predicting high beach-sand moistures, probably due to the increasing non-Lambertian nature of sand as the moisture content of the sand increased

Introduction

During the past ten years, remote sensing has been proven capable of delineating outcrop lithologies, a procedure often carried out in the early stages of mineral exploration. Typically, remote-sensing spectral data are compared to those in a reference library containing laboratory-acquired spectral data of individual minerals and rocks Through the use of a computer, correlations are made between the reference and remote-sensing spectra in an attempt to identify the surface material (Vincent, Thomson, and Watson, 1972).

In this investigation, beach sands were analyzed with the intent of determining not only mineralogy but also moisture and grain size These three parameters are of interest from both geological and engineering points of view. The mean grain size at a reference point on a beach is a fundamental characteristic of the beach. Studies have indicated that mean grain size is related to beach face slope (Komar, 1976), water percolation and permeability and ease of grain movement (Komar, 1977, Zenkovich, 1967, Huntley and Bowen, 1975, Fraser and Hester, 1977, Self, 1977). These factors play a major role in determining whether a beach

0034-4257/81/040295+16$02 50

will be erosional or depositional under different wave conditions (Madsen and Grant, 1976, Swart, 1976).

Additionally, recognition of these three sand parameters would also allow the identification of beach mineral deposits based on grain size and mineralogy. Since beaches are formed by intense erosion of the parent materials, more resistant minerals tend to be preserved and concentrated while others are dissipated. Depending on the origin of the sand, these residual minerals may be of economic value

In order to determine the mineralogy, moisture, and grain size of a given sand, a two-stage vector-length-decision and multiple linear regression approach was used This entailed the breakdown of mineralogy into five categories. Each category was then analyzed for moisture content and grain size using predictive multiple linear regressions based on selected spectral bands

Background

The theoretical basis for the work presented in this paper was developed over a period of approximately ten years. Studies have been made towards understanding the effects that grain size, moisture coating, and mineralogy of particulates have on reflected radiation from beach sands It was shown by Emslie (1966) and Aronson et al., (1967) that reflected radiation from beach sand is a function of. the wavelength of the radiation, the optical constants of the medium, i.e., n (refractive index) and k (index of absorption), the particulate grain size, the packing density, and the roughness of the surface. Hunt and Vincent (1968) used reflectance data based on ground laboratory samples to improve the work of Aronson et al The model of Hunt and Vincent also accounted for volume scattering of reflected radiation in sand particles.

Leu (1977) working at the Environmental Research Institute of Michigan (ERIM) collected beach sands (from Delaware) and measured their reflectance in the laboratory in the 0.4–2.5 μm range using a Cary 14 laboratory spectrophotometer. (The Cary 14 spectrophotometer is a device which is capable of digitally recording the reflectance spectrum of a surface in the 0.35—2.5 μm range) Leu then used multiple linear regression to correlate reflectance values in discrete reflectance bands to moisture and grain size. Leu's work showed promise, but his regressions did not work when beach sand reflectance values other than those from Delaware beaches were used This indicated the mineralogy of a beach sand strongly affects its reflectance spectra and that the effects of mineralogy must be understood before moisture and grain-size prediction algorithms can be run

In order to understand fully the effects of changes in mineralogy, moisture, and grain size on the spectral reflectance of beach sand, a sand-reflectance model was used. The model, an adaptation of the Suits radiative transfer vegetation canopy model, is known as AQUASAND (Suits, 1972). It uses, as inputs, the reflectance and transmittance for each mineral comprising the beach sand (i e , quartz, feldspar, magnetite, etc.). In addition, input to the model includes the sand grain size, the void space in the sand, and the moisture profile as a function of depth By varying these input parameters insight was gained into the effect of physical changes on the bulk sand reflectance

Using the information obtained from AQUASAND (Shuchman et al., 1978) the mineralogy, moisture, and grain-size

(MOGS) algorithm was developed using reflectance spectra measured on a Cary 14 spectrophotometer. These spectra ranged from 0.35–2.5 μm, an interval practical for existing remote sensing technology. The MOGS algorithm was evaluated both on the reflectance spectra from which it was derived and on spectra collected following the algorithm development. In addition, digital images of grain-size distribution were developed from actual multispectral scanner data.

Development of the MOGS Algorithm

The procedure of developing an algorithm to predict mineralogy, moisture, and grain size of beach sands was divided into three segments. First, a data base of sand-reflectance values was selected from which to build the algorithm, second, the necessary equations were developed, and third, the algorithm was evaluated using actual remotely sensed aircraft data.

All of the equations that make up the MOGS algorithm are based ultimately on 81 laboratory-measured reflectance spectra of beach samples obtained from a Cary 14 spectrophotometer operated by ERIM. The sand samples were collected from five diverse beach types located in various coastal areas of the continental United States between June 1974 and October 1978. The use of a large range of sand types was deemed necessary to give the MOGS algorithm a wide field of applicability. The mean grain size (diameter), moisture content, and approximate location of each beach sand sample used in the development of the MOGS algorithm are given in Table 1.

From inspection of both the AQUASAND-generated and empirical spectra, it became apparent that mineralogy had by far the greatest influence on the reflectance spectra. So great is this influence that it tends to mask the more subtle features of changes in grain size and, to a much lesser extent, moisture.

In order to achieve the fine detail needed for the classification of moisture and grain size while still maintaining the applicability to a large range of mineralogies, a two-stage procedure was established in the development of the MOGS algorithm (Fig. 1). The first stage entails a breakdown of sand mineralogy into discrete classes. Within each class, second-stage multiple linear regressions were used to derive the moisture and grain-size information. Using this method the second-stage regressions do not have to account for the large spectral effects of mineralogy characteristic of diverse beach sands. This division increased the accuracy and predictive ability of the moisture and grain-size regression equations considerably.

In order to determine which spectral regions would best be able to differentiate and predict the parameters of interest, the AQUASAND beach sand model was used. By varying the model input parameters in a logical fashion it was possible to predict which regions of the spectrum yielded the most useful information. These spectral regions were then used in the MOGS algorithm to predict the parameters of interest. Because the MOGS algorithm is to be used on aircraft-collected multispectral scanner (MSS) data, all the input spectral data were divided into 17 spectral "bands" which are feasible (dictated by atmospheric transmittance) for implementation using existing MSS technology (Table 2). In any given portion of the MOGS algorithm only a subset of these 17 bands were used, as will be shown later.

TABLE 1 The Mean Grain Sizes and Moisture Contents of the 81 Sand Samples Used in the Development of the MOGS Algorithm. Samples are given by mineralogical class

Sand I.D.*	Moisture Content (%)	Mean Grain Size (mm)
A1	4.5	0.35
A2	29.4	0.35
A3	15.0	0.37
A4	28.4	0.50
A5	11.3	0.43
A6	33.4	0.32
A7	13.1	0.35
A8	24.9	0.38
A9	8.8	0.44
A10	29.7	0.43
B1	21.0	0.40
B2	24.6	0.76
B3	14.2	0.46
B4	27.2	0.88
B5	11.0	0.63
B6	19.0	0.95
B7	6.8	0.71
B8	24.9	0.76
B9	6.2	0.71
B10	21.3	0.71
B11	20.0	0.81
B12	34.0	0.69
B13	6.0	0.55
B14	31.0	0.83
B15	18.0	0.67
B16	32.0	0.57
B17	18.0	0.56
B18	23.0	0.65
B19	3.0	0.94
B20	23.0	0.60
M1	5.0	0.36
M2	15.0	0.36
M3	25.0	0.36
M4	30.0	0.36
M5	5.0	0.41
M6	15.0	0.41
M7	0.0	0.23
M8	0.0	0.29
M9	0.0	0.41
M10	0.0	0.36
M11	10.0	0.23
M12	25.0	0.23
M13	30.0	0.23
M14	10.0	0.41
M15	20.0	0.41
M16	15.0	0.23
M17	22.0	0.28
M18	2.0	0.31
M19	8.0	0.26
H1	0.0	0.32

TABLE 1 (continued)

Sand I.D.*	Moisture Content (%)	Mean Grain Size (mm)
H2	5.0	0.32
H3	10.0	0.32
H4	15.0	0.32
H5	20.0	0.32
H6	25.0	0.40
H7	30.0	0.40
H8	35.0	0.40
H9	0.0	0.17
H10	15.0	0.22
H11	10.0	0.32
H12	5.0	0.40
MX1	25.0	0.22
MX2	0.0	0.22
MX3	10.0	0.22
MX4	15.0	0.22
MX5	30.0	0.22
MX6	35.0	0.22
MX7	20.0	0.22
MX8	5.0	0.22
MX9	16.0	0.22
MX10	4.0	0.22
MX11	10.0	0.22
MX12	29.0	0.22
C1	0.0	$\sim 1\times1\times0.25$
C2	10.0	$\sim 1\times1\times0.25$
C3	5.0	$\sim 1\times1\times0.25$
C4	20.0	$\sim 1\times1\times0.25$
C5	15.0	$\sim 1\times1\times0.25$
C6	30.0	$\sim 1\times1\times0.25$
C7	25.0	$\sim 1\times1\times0.25$
C8	40.0	$\sim 1\times1\times0.25$
C9	50.0	$\sim 1\times1\times0.25$

*A = Indian River Inlet, Delaware
B = Delaware Bay, Delaware
M = Michigan Coastline (Sleeping Bear State Park, Petosky State Park, Mason–Oceana County Line, Pentwater State Park, and Muskegon State Park)
H = South Beach and Glen Eden Beach Oregon Coastline
MX = Panama City, Florida (Gulf of Mexico)
C = Marine Carbonate, Florida Keys

The prediction of mineralogy

Rather than attempting to predict the individual mineral components of the different sands it was decided that grouping the sands into homogeneous types would

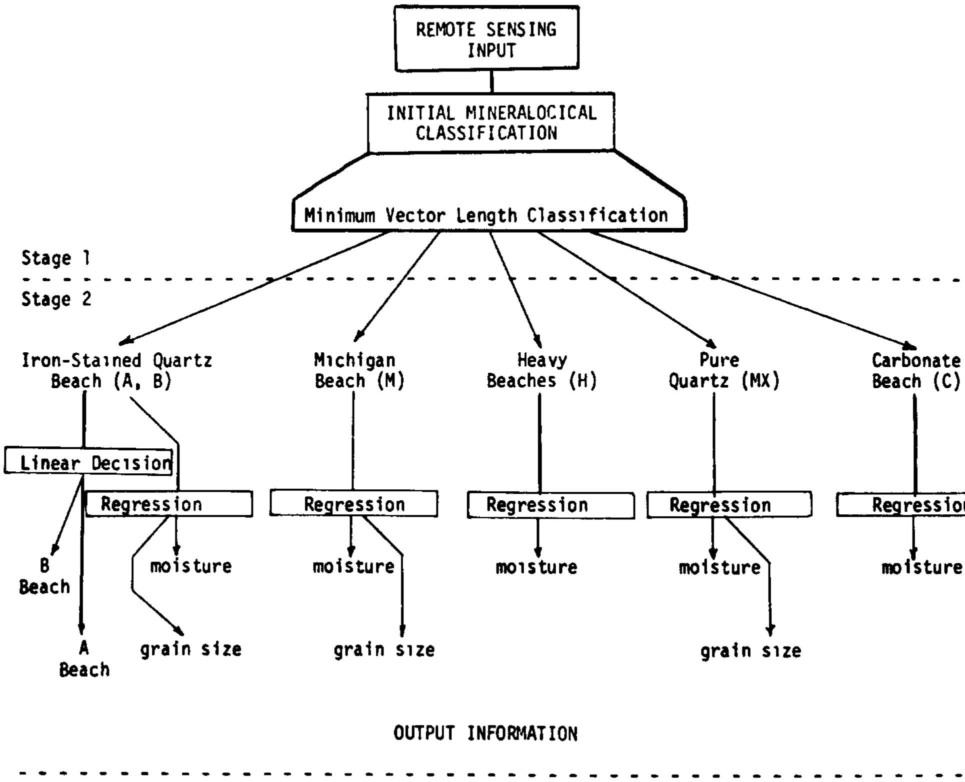

FIGURE 1 Flow diagram of the MOGS algorithm

TABLE 2 The 17 Spectral Bands Used in the Development of Moisture and Grain Size Regression Equations

Band Number	Wavelength Range (μm)
1	0 43–0 47
2	0 47–0 49
3	0 49–0 51
4	0 51–0 53
5	0 53–0 56
6	0 56–0 59
7	0 59–0 63
8	0 63–0 67
9	0 70–0 75
10	0 75–0 80
11	0 80–0 90
12	0 90–1 00
13	1 00–1 10
14	1 10–1 20
15	1 20–1 35
16	1 50–1 85
17	2 10–2 50

be more productive. As such, five groups were defined which, for the most part, corresponded with the geographic location of collection of the data base samples. The five mineralogical classes are as follows:

1. Iron-stained Atlantic coast type (A,B),
2. Iron-stained Michigan type (M),
3. Non-iron-stained pure quartz type (MX),
4. Heavy mineral (dark sand) type (H),
5. Carbonate type (C).

Typical spectra of these five mineralogical categories is given in Shuchman et al. (1978) To discriminate the five mineralogical classes a minimum-vector-length decision framework was used The concept is developed as follows. Suppose that there are two points, A and B, located in two-dimensional space. The distance, or vector length, L, from A to B can be expressed in terms of the X and Y locations of points A and B as

$$L=\left[(X_A-X_B)^2+(Y_A-Y_B)^2\right]^{1/2} \quad (1)$$

This is, of course, related to the Pythagorean Theorem. Now suppose we have a p-dimensional system with A and B located in each dimension. The vector length can be expressed as

$$L=\left(\sum_{i=1}^{p}(X_{iA}-X_{iB})^2\right)^{1/2}, \quad (2)$$

where X_{iA} is the location of point A in the ith dimension and X_{iB} is the location of point B in the ith dimension.

This rationale can be used to classify some point, T, as being the member of one of n classes $(A_j, j=1, n)$, by finding the minimum vector length from T to A_j $(j=1, n)$. In other words T is said to be a member of the class which is closest to it, on the average, across all p dimensions. The minimum vector length is defined as

$$L_{\min}=\min_{j=1,\ldots,n}\left(\sum_{i=1}^{p}(X_{iT}-X_{iA_j})^2\right)^{1/2} \quad (3)$$

Notice that Eq. (3) has no provision for variability in the n classes, therefore, $L_{\min}$ is chosen as being the shortest linear vector length. If each class has the same variability associated with it this causes no difficulty. In this experiment, however, there were considerable differences in variability between the classes so that a modification of Eq. (3) had to be made The standard deviation (SD) was used to modify the distance between T and A_j related to each dimension thus removing the effects of variability from each class. This normalized minimum distance equation is expressed as

$$L_{\min}=\min_{j=1,\ldots,n}\left[\sum_{i=1}^{p}\left(\frac{X_{IT}-X_{iA_j}}{\mathrm{SD}_{ij}}\right)^2\right]^{1/2}, \quad (4)$$

where SD_{ij} is the standard deviation associated with the jth class in the ith dimension.

In the application of this method to the classification of mineralogy, the "dimensions" are spectral bands or ratios of spectral bands and the "classes" are mineralogical types. Eight spectral bands (Table 3) and all possible unique ratios of those spectral bands were used to classify the mineralogical type of an input sand as one of five categories. The object was to make each category as homogeneous as possible so that the moisture and grain-size regressions which followed would be sensitive to small scale spectral changes.

The prediction of moisture and grain size

Using the AQUASAND model, we found that information related to moisture content of sands is best derived from the spectral region beyond 1.0 μm. This is the result of the spectral reflectance of sand in this region being reduced by absorption in proportion to the amount of water present. (Exceptionally high spectral absorption is noted near 1.4 and 1.9

TABLE 3 The Eight Spectral Bands Used in the Breakdown of Beach Mineralogy into One of Five Categories. In addition to these eight bands all unique ratio combinations were also used

Band Number	Wavelength Range (μm)
1	0.43–0.47
2	0.47–0.49
3	0.51–0.53
4	0.53–0.56
5	0.59–0.63
6	0.80–0.90
7	0.90–1.0
8	1.0–1.1

μm.) Although the spectral reflectance in these regions is highly correlated to moisture we did not consider them since atmospheric absorption prohibits their use by an airborne sensor.

Changes in grain size seem to manifest themselves most clearly in the shorter wavelengths (0.4–0.7 μm). Grain-size information is gained by light being reflected from sand grains below the surface through surface grains. The transmittance through the surface grains is reduced by internal scattering and absorption of the particle. Since both of these factors are dependent on thickness, the bulk reflectance of a sand is dependent to some degree on the grain size. Theoretically, a coarse-grained sand should have a lower reflectance than a fine-grained sand of the same mineralogical composition, surface frosting, and with similar moisture content. According to our measurements this appears to be the case.

This grain-size phenomenon can be confounded in two ways. First, if there is no scattering or absorption within the grains (i.e., a perfectly clear material at all wavelengths) there can be no attenuation. Fortunately, even in our purest quartz sands there were enough impurities and inclusions to give some attenuation. Second, the sand grains may be opaque and thus attenuate too much light. This appears to be the case in the heavy mineral and carbonate beaches. Most of the bulk reflectance for these two types was the result of surface reflectance and essentially none from light transmitted through the surface grains from below. We were unable to create accurate grain-size equations for these types.

Utilizing the physical phenomena discussed above we are able to develop multiple linear regression equations for predicting moisture in all five mineralogical classes and grain size for three of the five mineralogical classes. The basis for all the regressions, except one, was the sample group corresponding to a given mineralogical class. The single exception was the grain-size equation corresponding to a pure quartz beach. Our samples within this type consisted of a single grain size (0.22 mm) and, as such did not provide an adequate basis for regression equations. For this case, we used AQUASAND-generated spectra to simulate a wide range of grain sizes in order to add grain-size variability to the data set.

Seventeen spectral bands between 0.4 and 2.5 μm were chosen for use in the regressions (Table 2). Within the 17 bands, only those which were predicted by the AQUASAND model to be most informative were used. In this way we could be reasonably certain that the regression equations would respond the correct parameter and thus yield accurate predictions. The predictive equations together with the associated standard errors (SE), and coefficient of variation (R^2) are given in Table 4.

In summary, the MOGS algorithm represents (see Fig. 1) a computer-controlled package of equations. The input is a set of 17 spectral reflectance bands obtained

TABLE 4 Multiple-Linear-Regression Equations for the Prediction of Moisture and Grain Size The equations are listed by mineralogical class Grain size is in mm

A	Iron-stained quartz[a] — Atlantic coast
	Predicted moisture $\% = 67\ 964 - 65\ 046 \left(\frac{\text{Band } 16}{\text{Band } 14}\right)$
	SE $= \pm 3\ 08\%$, $R^2 = 0\ 888$
	Predicted grain size $= 6\ 87 - 3\ 4634\ (\text{Band } 7)^{1/4} + 0\ 0300\ (\text{Band } 1) + 0\ 01672\ (\text{Band } 15)$
	SE $= \pm 0\ 13$ mm, $R^2 = 0\ 603$
B	Iron-stained quartz–Michigan coast
	Predicted moisture $\% = 60\ 149 - 49\ 961 \left(\frac{\text{Band } 16}{\text{Band } 11}\right) - 2\ 226 \left(\frac{\text{Band } 17}{\text{Band } 1}\right)$
	SE $= \pm 2\ 56\%$, $R^2 = 0\ 970$
	Predicted grain size $= 0\ 6405 - 0\ 0152\ (\text{Band } 5) - 0\ 0047\ (\text{Band } 17)$
	SE $= \pm 0\ 055$ mm, $R^2 = 0\ 558$
C	Non-Iron-stained quartz
	Predicted Moisture $\% = 127\ 02 - 65\ 159 \left(\frac{\text{Band } 16}{\text{Band } 15}\right) - 64\ 065 \left(\frac{\text{Band } 15}{\text{Band } 14}\right)$
	SE $= \pm 2\ 12\%$, $R^2 = 0\ 971$
	Predicted grain size $= 1\ 158 - 2\ 328\ (\text{Band } 10) + 0\ 3201 \left(\frac{\text{Band } 7}{\text{Band } 1}\right) + 0\ 2858\ (\text{Band } 10)$
	SE and R^2 not applicable
D	Carbonate
	Predicted moisture $\% = 596\ 28 - 642 \left(\frac{\text{Band } 14}{\text{Band } 17}\right) - 1\ 081\ (\text{Band } 14) + 0\ 1538\ (\text{Band } 17)$
	SE $= \pm 4\ 09\%$, $R^2 = 0\ 879$ No grain-size equation
E	Heavy mineral
	Predicted moisture $\% = 19\ 284 + 11\ 194 \left(\frac{\text{Band } 14}{\text{Band } 17}\right) - 1\ 081\ (\text{Band } 14) + 0\ 1538\ (\text{Band } 17)$
	SE $= \pm 4\ 09\%$, $R^2 = 0\ 879$ No grain-size equation

[a] Iron-stained quartz was determined by visual examination under stereomicroscope

from an unknown sand. Based on these bands, the sand is classified as being a member one of five mineralogical types. Depending on the mineralogical type, the appropriate moisture and grain-size (where applicable) equations are applied to the data. The output from the MOGS algorithm is the predicted mineralogical class, the predicted moisture, and the predicted grain size.

Test Results of the MOGS on Laboratory Spectra

The MOGS algorithm was first tested on 70 of the 81 samples from which it was derived and the results were very promising. Eleven samples were discarded because their grain sizes were abnormally large or percentage of moisture was inaccurate. The classification of mineralogy was 99%+ correct. The overall correlation of predicted to actual moisture was 96% (significant at the 0.001 level) and the overall correlation of predicted to actual grain size was 88% (significant at the 0.001 level). However, testing any equation or algorithm on the samples from which it was derived is not conclusive. For this reason the MOGS algorithm was tested on several other beach sand samples which were independently collected and spectrally measured following the algorithm construction. These results are given in Table 5. In each case, the MOGS algorithm selected a mineralogy which allowed the moisture and grain-size regression to operate correctly The independent test yielded an actual moisture to predicted moisture correlation of 0.95 (significant at the 0 01 level) The prediction of grain size was in

TABLE 5 Comparison of Actual Parameters to Predicted Classifications by the MOGS Algorithm Samples used here were collected independently of those on which the algorithm is based

Sample Mineralogy		Moisture (%)			Mean Grain Size (mm)		
Actual	Predicted	Actual	Predicted	% Different	Actual	Predicted	(mm) Different
MICH1	MICH	37 7	25 6	−12 1	0 26	0 28	+0 02
MICH2	MICH	3 2	3 7	+0 5	0 28	0 30	+0 02
MICH3	MICH	0 3	0 0	−0 3	0 25	0 32	+0 07
MICH4	MICH	12 1	16 0	+3 9	0 23	0 29	+0 06
MICH5	MICH	15 0	12 7	−2 3	0 25	0 30	+0 05
MICH6	MICH	28 0	26 2	−1 8	0 28	0 29	+0 01

no case more than 0 07 mm different from the actual grain size.

Test of the MOGS Algorithm on MSS Data

The next logical test for the MOGS algorithm was to evaluate it on actual multispectral scanner (MSS) data. Such an investigation was carried out using aircraft data obtained from the ERIM-MSS. The ERIM-MSS (Hasell et al, 1974) is an optical scanning device, i.e , it receives signals continuously while the sensor instantaneous field of view (IFOV) moves over the flight path scanning the terrain The MSS is a passive device, meaning it senses energy originating from the sun and reflected from the terrain. The data from the MSS used in this analysis covered 12 discrete spectral bands in the 0.4–2.5 μm region of the electromagnetic spectrum (see Table 6)

TABLE 6 Spectral Bands Used by ERIM–MSS for Testing the MOGS Algorithm

Band Number	Range (μm)
1	0 40–0 44
2	0 43–0 46
3	0 45–0 49
4	0 48–0 53
5	0 51–0 57
6	0 54–0 63
7	0 60–0 72
8	0 66–0 84
9	0 78–1 1
10	1 2–1 4
11	1 5–1 8
12	2 0–2 6

Field test

Multispectral Scanner data were collected over three test sites along the Michigan shoreline; Muskegon State Park, Pentwater State Park, and Mason–Oceana (M–O) County line. The flight, part of an ERIM flight test for a NASA and NOAA program, took place on 1 November 1978 under clear skies between 1:00 and 2:00 P M.

Coincident with the fly-over, the following ground truth survey was carried out at the Pentwater test site.

1. Sand samples were collected to confirm grain size and moisture conditions at the time of flight, and
2. Reflectance panels (black and gray) were placed on the beach and radiance and irradiance spectral measurements obtained.

Additionally, three sand samples were taken at the M–O County line site and two sand samples obtained along with a reflectance measurement at the Muskegon State Park test site

The Michigan beach test was the first test of the MOGS algorithm on actual MSS data. The bands available on the ERIM–MSS (M7) as it presently functions necessitated a change in the band classification using the MOGS algorithm. The algorithm was changed to handle a total of 12 instead of 17 bands. This was simply done by truncating the five bands from the algorithm not available on the ERIM-MSS (M7). The resulting predictions of mineralogy using 12 instead of 17 were not affected. Using only five bands and ten ratios, the algorithm classified the mineralogies very well. This indicates that the use of eight bands and 26 ratios, as in the original algorithm, is probably over precision. In addition, the M7 bands give very nearly the same predictions for moisture and grain size for the Michigan beaches as the 17 bands which were used to develop the original equations.

Aircraft MSS data reduction

Table 6 lists the 12 channels of MSS data used in the Michigan tests. These channels (as mentioned previously) were selected as being very close to the channels used in the development of the MOGS algorithm. The nine channels corresponding to the shorter wavelengths utilized a photomultiplier detection system while the three longer wavelength channels used an InSb detector. The data were recorded digitally on a High Density Digital Tape (HDDT) for later computer processing.

Using an ERIM computer video display, the exact location of the test sites were determined and the data for all three test sites were transferred to a computer-compatible tape (CCT) for use on the University of Michigan AMDAHL 470 computer system (MTS). Rather than converting all the data, only an area 100 pixels on either side of the test site was recorded for each test site. Each pixel for the test data (600 m altitude) is approximately a 1.5 m square The use of only 100 pixels on either side of the test site negated having to correct the aircraft data for scanning angle effects of the sensor

Using the generated CCT on MTS, gray maps (computer-generated images) were produced to ascertain the exact areas from which the sand samples were collected. Upon specific location of the sample areas within the test site, the actual digital values obtained by the remote sensor were extracted. The data values obtained from MTS corresponding to the sample areas were then tabulated and "calibrated" This was accomplished by using an MTS module to extract the calibration values related to each scan line which contained a sample point. The "blackbody" calibration value was subtracted from the sample value for each sample to normalize the data. We found essentially no variability between scan lines in terms of the calibration values.

Concurrent with the data extraction, the sand samples obtained from the test site were measured for reflectance using the Cary 14 spectrophotometer. The signal values obtained from the scanner data were then plotted against the appropriate band reflectance, as measured with the Cary 14, to achieve a signal value to reflectance transfer curve For some reason, probably related to the non-Lambertian nature of objects in the scene, the relationship did not appear to be strictly linear in all bands. This nonlinearity appears to be most pronounced for the near infrared spectral bands which use the InSb detector. In addition, the reflectance calibration panels which were deployed at the Pentwater Site do not plot well with the sand values. This means that, in this case, the panels were not particularly useful in calibrating the MSS system to values of reflectance. Our final signal-value-to-surface reflectance calibration was accomplished using the reflectance of a few sand samples (four) plotted against the MSS digital signal value. The digital values of other areas on the beach were then altered to reflectance using these curves. Thus the ERIM-MSS (M7) received radiance value was converted to a reflectance value using this technique.

Aircraft test results

The test results using the aircraft scanner data are encouraging (Table 7). The correlation (R) of predicted to actual moisture content is 0.91 (significant at the 0.01 level) and the prediction of grain size is, in no case, greater than 0.09 mm different from the actual grain size. The predicted grain sizes shown in Table 7 are all larger than the actual measured grain size. The statistical analysis on the sand samples used to create the Michigan grain-size regression equation showed the sands to be moderate to well sorted (i.e., low standard deviation of grain size) but exhibiting a negative skewness in almost all cases This negative skewness, indicative of a coarse fraction, could have biased the grain-size prediction algorithm and caused the larger than actual prediction of grain size to result.

The moisture prediction appears particularly poor for high moisture contents. This is most likely the result of wet sand at the test sites exhibiting bidirectional dependencies (i.e., a failure to behave in a Lambertian manner). These bidirectional characteristics are enhanced at low sun angles and are not accounted for by the MOGS algorithm. Although the flight took place at 1.30 EST the sun was only 38° above the horizon on November 1.

A laboratory experiment was conducted to quantify the effects of bidirectional dependencies of wet sand. Figure 2 shows the laboratory set-up used to conduct the test. The sand was spread evenly in a 70×70 cm tray to a depth of 2 5 cm Illumination was provided by a 200-μW projector lamp whose beam was optically collimated to provide a highly directional source (i e, $\simeq 6°$) The detector used was

TABLE 7 Comparison of Actual Parameters to Predicted Classifications by the MOGS Algorithm The sand spectra used here were collected by the ERIM–MSS

Sample Mineralogy		Moisture (%)			Grain Size (mm)		
Actual	Predicted	Actual	Predicted	% Different	Actual	Predicted	mm Different
Pentwater	MICH	22 3	12 1	−10 2	0 25	0 32	+0 07
Pentwater	MICH	1 0	0 0	−1 0	0 23	0 28	+0 05
Pentwater	MICH	8 0	10 1	+1 9	0 22	0 25	+0 03
Pentwater	MICH	28 0	16 9	−11 1	0 26	0 35	+0 09
Pentwater	MICH	5 0	2 2	−2 3	0 24	0 26	+0 02
M–O Line	MICH		Not measured		0 29	0 32	+0 06
M–O Line	MICH		Not measured		0 27	0 36	+0 09
M–O Line	MICH		Not measured		0 29	0 37	+0 08
Muskegon State Park	MICH		Not measured		0 25	0 30	+0 05

a Coherent Optics power meter which utilized a silicon detector. The aperture of the detector was reduced using baffles such that an area approximately 5 cm square on the sand surface was sensed. To avoid having the detector head shadowing the sand it was offset such that it was viewing at an angle of 23° from the vertical As is shown in Fig 2, the lamp was moved through several angles from normal to the sand surface to nearly parallel with it At each angle the flux to the detector was measured and recorded.

According to theory, if a surface is perfectly Lambertian then the exitance from the surface should decrease with the cosine of the angle of incidence. Therefore the exitance observed at any illumination angle should be equal to the exitance with the illumination normal to the surface multiplied by the cosine of the angle of interest. Using this relationship, a useful measure of the Lambertian nature of a material is

$$R = \frac{M_\theta}{M_0 \cos\theta}, \tag{5}$$

where R is the measure of Lambertian nature, M_θ is the exitance observed at illumination angle θ and M_0 is the exitance observed with the illumination normal to the surface. For a perfectly Lambertian material R should be 1 0 for all θ If R is less than 1.0 then less flux is being reflected at angle θ than was expected, and if R is greater than 1.0 the reverse is true

Using the experimental design just described, two sand conditions were investigated. dry sand and sand with ~25% moisture As can be seen in Fig 3(a), dry sand is quite Lambertian in character at angles up to 60° incident (30° above the horizon). The sun angle during the Michigan test flight was approximately 52° incident indicating the exitance from dry sand was ~84% of that expected from a Lambertian material. This is in fact quite good for this incidence angle although a more nearly normal incidence angle (higher sun) would have been desirable

The wet sand [Fig. 3(b)] exhibits strong bidirectional properties indicative of a

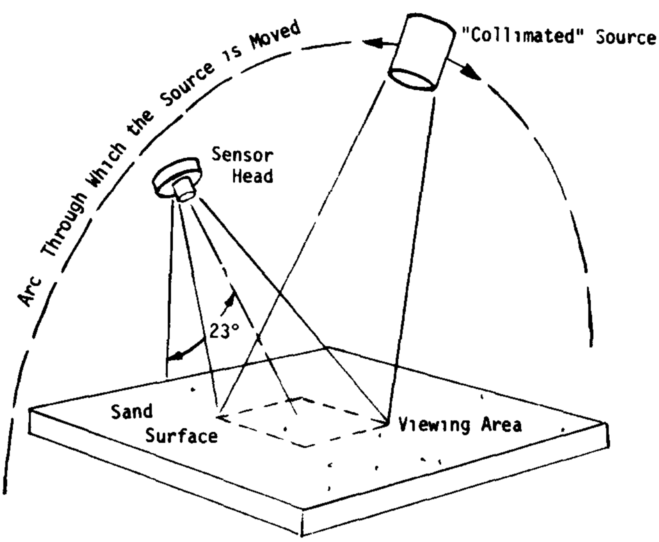

FIGURE 2 Experiment set-up used to determine Lambertian properties of sand

semispecular surface. The raw data indicates a very high exitance at 0° incidence followed by a rapid fall off at other incidence angles relative to that observed for dry sand. The implication is that there is a specular return at 0° incident—a very non-Lambertian characteristic, for such a case the assumption of a Lambertian surface does not hold. Note from Fig. 3 that for sun angle ±15° from zenith wet and dry sands decreased in reflectance approximately the same amount and therefore minimize non-Lambertian effects. It should be noted that the goniometric study described was not a spectral study but rather used a light source that ranges the visible and is weighted to the infrared.

In summary, the Cary 14 Spectrophotometer makes a reflectance measurement that is hemispherical, i.e., the reflectance properties whether bidirectional, Lambertian, or diffuse have little bearing on the reflectance that is sensed. Conversely, the MSS only intercepts radiation which is reflected in a certain direction as opposed to the diffuse sensing of a spectrophotometer For an MSS, this sensing is normal

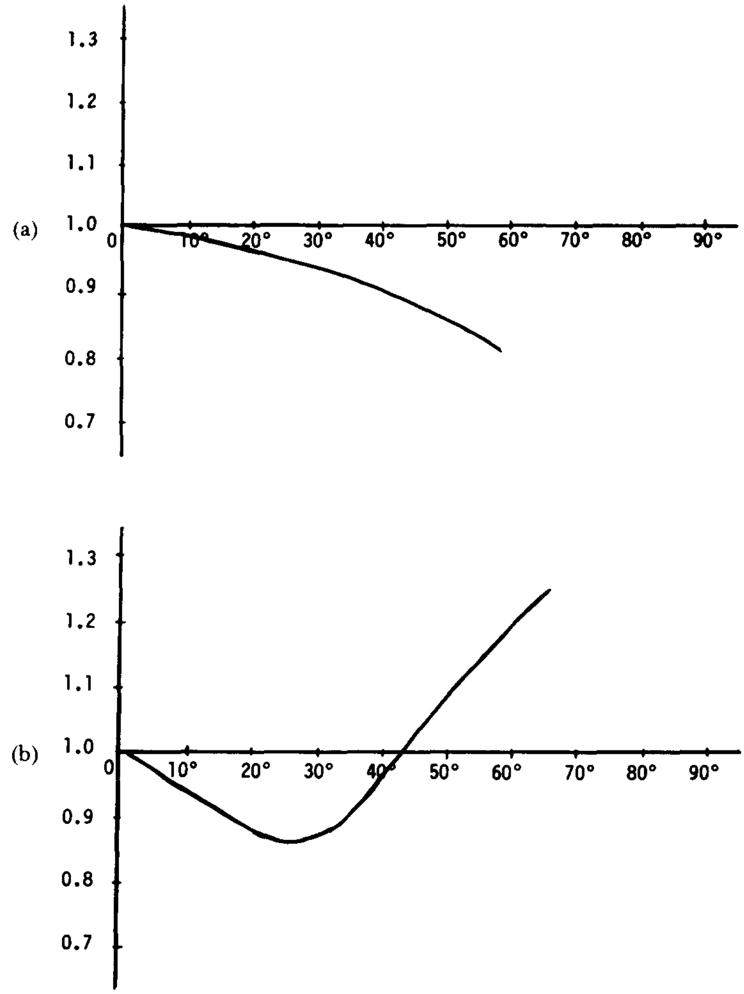

FIGURE 3 (a) Dry sand case (b) Wet sand case

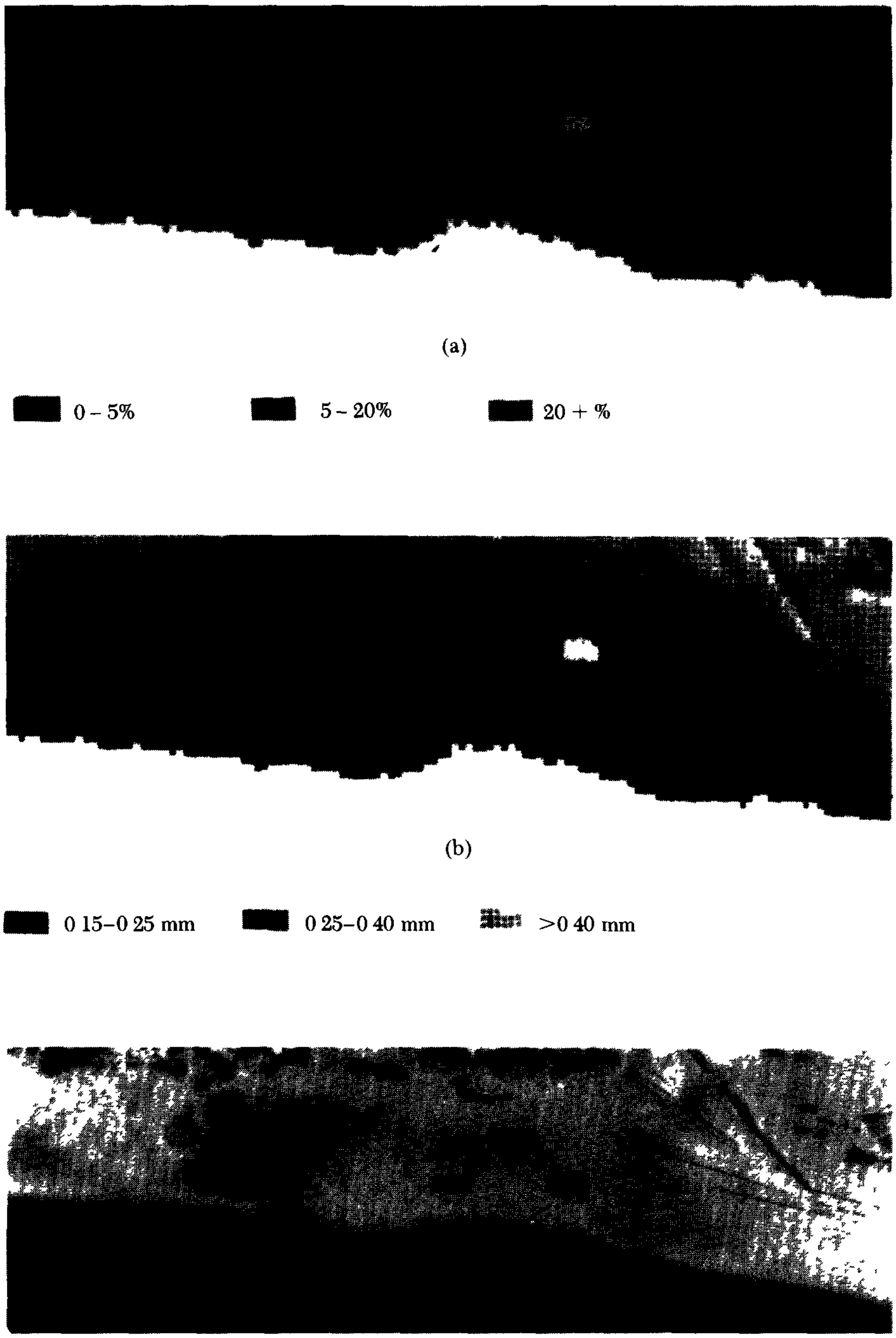

FIGURE 4 Digital imagery, generated by the MOGS algorithm showing the distribution of moisture and grain size on Pentwater Beach (Pentwater State Park, Michigan). White areas are either unclassified regions or open water. Lighter shade indicates higher moisture content. (a) Moisture distribution image. (b) Grain-size distribution image. (c) Panchromatic aerial photograph.

to the sensed surface at the center of the scan and progressively more oblique toward the edges of the scan The type of illumination is highly variable ranging from diffuse with an overcast sky to nearly specular on a clear sunny day. In the former case, the geometry is much like that of a spectrophotometer in reverse—diffuse source and specular sensing Because of reciprocity the apparent reflectance as derived from MSS data, ignoring path radiance factors, should be exactly the same as the reflectance sensed by a spectrophotometer Thus, to minimize bidirectional reflectance, future aircraft flights should be made during complete midaltitude (3000 m) cloud cover or sunny skies with the sun close to the zenith (summer sun) as indicated from Fig. 3

Applying the same moisture and grain-size equations used in the previous analysis, the entire Pentwater State Park beach on a pixel-by-pixel basis (in this case 1 5 m × 1.5 m) was classified with respect to grain size and moisture content The two MOGS-generated digital maps (see Fig. 4) show the predicted moisture and grain-size distribution on the beach at Pentwater. Also included on Fig. 4 is a panchromatic aerial photograph take coincident with the MSS data. The ground truth measurements taken at the time of flight correlate well with these images. Figure 4 helps to demonstrate how an entire sandy coastline might be analyzed in respect to moisture, grain size, and gross mineralogy using a small subsection as calibration

Conclusion

The development of the MOGS algorithm has demonstrated the feasibility of obtaining quantitative moisture and grain-size information from the spectral reflectance of beach sands. The determination of grain size is dependent on the sand grains being neither opaque nor perfectly clear.

The two stage nature of the MOGS algorithm is directly responsible for its broad applicability without loss of detail. By separating the mineralogical types prior to the prediction of moisture and grain size much of the variability which could easily hide small scale changes is removed. The use of a vector-length discriminant function to classify mineralogy worked extremely well in this application, since 36 different dimensions could be evaluated simultaneously. A multistage approach involving multiple classification techniques is a powerful tool, one which may be very useful in many areas of remote sensing.

The Lake Michigan field test has further demonstrated the MOGS algorithm's applicability to remotely sensed field data Grain size was predicted to within 0 09 mm mean diameter of the actual size while beach moistures below 20% were accurately predicted In all cases, the computer algorithm correctly identified the Michigan beach mineralogy as being a predominately iron-stained quartz–feldspar beach.

This work was supported by the Office of Naval Research (ONR) contracts N0014-74-C-0273 and N-0014-78-C-0458. Mr. Hans Dolezalek of ONR served as the technical monitor on both contracts. The Rackham Graduate School, The University of Michigan supported the collection of beach sands along Lake Michigan and the ensuing laboratory analysis of the sand parameters. Ms. Karla Amble of ERIM performed the majority of the laboratory analysis of the sand parameters

Mr. Carl Davis, formerly of ERIM, now with Eaton Stamping Company, is acknowledged for creating, as well as operating, the computer software necessary to perform this research.

The authors would like to thank Dr. Gwynn Suits, Mr. Fred Thomson, and Dr. Philip Jackson of ERIM for their guidance and critical review of the work presented in this paper. Ms. Kathleen Newstead of ERIM is thanked for her typing of the manuscript.

References

Aronson, J R , Emslie, A G., Allen, R. V , and Mc Linden, H. G , (1967), Studies of the middle- and far-infrared spectra of mineral surfaces for application in remote compositional mapping of the moon and planets, *J Geophys. Res* 72.687–703.

Emslie, A G (1966), Theory of diffuse spectral reflectance of a thick layer of absorbing and scattering particles, in thermophysics and temperature control of spacecraft and entry vehicles In *Progress in Astronautics and Aeronautics, Vol. 18*, (G B Heller, ed), Academic, New York

Fraser, G S and Hester, N C (1977), Sediments and sedimentary structures of a beach-ridge complex, southwestern shore of Lake Michigan *J Sed Petrol* 47 1187–1200

Hasell, P. G et al (1974), Michigan experimental multispectral mapping system. A description of the M7 airborne sensor and its performance, Technical Report 190900-10-T ERIM, Ann Arbor, MI

Hunt, G R. and Vincent, R. K. (1968), The behavior of spectral features in the infrared emission from particulate surfaces of various grain sizes. *J Geophys Res*. 73.6039–6046

Huntley, D A and Bowen, A J (1975), Comparison of the hydrodynamics of steep and shallow beaches in (J Hails and A Carr, eds.) *Nearshore Sediment Dynamics and Sedimentation*, John Wiley & Sons, New York, pp 69–109

Komar, P D (1976), *Beach Processes and Sedimentation*, Prentice-Hall, Inc., Englewood Cliffs, NJ, 429 p

Komar, P D (1977), Selective longshore transport rates of different grain-size fractions within a beach *J Sed. Petrol* 47.1444–1453

Leu, David J (1977), Visible and near-infrared reflectance of beach sands. a study on the spectral reflectance/grain size relationship *Remote Sensing Environ* 6.169–182

Madsen, O S. and W D Grant (1976), Quantitative description of sediment transport by waves in *Proceedings of the 15th Coastal England Conference*, Am Soc Civil Eng , New York, 1093–1112

Self, R. P. (1977), Longshore variation in beach sands, Nautla area, Veracruz, Mexico, *J Sed Petrol* 47 1437–1443.

Shuchman, R. A , Suits, G. H , and Davis, C F (1978), AQUASAND A beach reflectance model and validation tests in *Proceedings of Fifth Canadian Symposium on Remote Sensing of Environment*, Victoria, B C , Canada

Suits, G H (1972), The calculation of the directional reflectance of a vegetation canopy *Remote Sens Environ* 2.117–125

Swart, D H (1976), Predictive equations regarding coastal transports in *Proceedings of the 15th Coastal England Conference* Am Soc Civil Eng , New York, pp 1113–1132

Vincent, R K , Thomson, F J , and Watson, K (1972), Recognition of exposed quartz sand and sandstone by two-channel infrared imagery *J Geophys Res* 77 2473–2477

Zenkovich, V P. (1967), *Processes of Coastal Development*, Interscience, New York, 738 p

Received 29 March 1980, revised 25 February 1981